Biological Conservation 258 (2021) 109147

Contents lists available at ScienceDirect

Biological Conservation

journal homepage: www.elsevier.com/locate/biocon

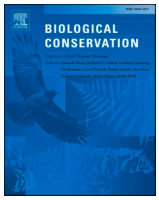

Integrating harvest and camera trap data in species distribution models

Neil A. Gilbert [a,*], Brent S. Pease [b], Christine M. Anhalt-Depies [c], John D.J. Clare [a,d], Jennifer L. Stenglein [c], Philip A. Townsend [a], Timothy R. Van Deelen [a], Benjamin Zuckerberg [a]

[a] Department of Forest and Wildlife Ecology, University of Wisconsin-Madison, 1630 Linden Drive, Madison, WI 53706, USA
[b] Department of Forestry and Environmental Resources, North Carolina State University, 2800 Faucette Drive, Raleigh, NC 27695, USA
[c] Wisconsin Department of Natural Resources, 2801 Progress Road, Madison, WI 53716, USA
[d] Museum of Vertebrate Zoology, University of California, Berkeley, 3101 UC Berkeley Road, Berkeley, CA 94270, USA

ARTICLE INFO

Keywords:
Citizen science
Data fusion
Hierarchical modeling
Joint-likelihood
Jurisdictional observation network
Species-environment relationships
Wildlife management

ABSTRACT

Wildlife managers need reliable information on species distributions (i.e. patterns of occurrence and abundance) to make effective decisions. Historically, managers have relied on harvest records (collected at broad spatial extents but coarse resolution) to monitor wildlife populations. However, emerging citizen-science datastreams can potentially supplement harvest-based monitoring by providing fine-resolution data that permit identification of species-environment relationships needed to predict occurrence and abundance. We combined harvest records and citizen-science camera-trap data in integrated species distribution models (iSDMs) to estimate species-environment relationships and distribution patterns of six wildlife species in Wisconsin, USA. We expected that iSDMs would more precisely estimate species-environment relationships and predict spatial abundance patterns intermediate between camera- and harvest-only SDMs. We also conducted simulations to explore the consequences of incomplete knowledge of harvest effort for estimates of abundance and species-environment relationships. Integrated models produced more precise species-environment relationships than camera-only models in 53% of the relationships we tested; all harvest-only models failed to converge. Moreover, integrated and camera-only models showed low agreement (mean: 19.67%) in identifying abundance "hotspots" but considerably higher agreement (mean: 45.17%) in identifying abundance "cold spots". Our simulations showed that abundance patterns estimated by iSDMs may suffer from imprecision if harvest effort is poorly measured. We recommend that harvest records be collected at finer spatial resolutions and be paired with in-depth effort reporting. Our work demonstrates the potential for integrating an existing datastream (harvest records) with an emerging one (citizen-science camera-trap monitoring) for modeling species distributions and providing support for wildlife management decisions.

1. Introduction

Effective wildlife management requires knowing where focal species are and are not found. Thus, managers often predict spatial occurrence and abundance patterns based on ***species-environment relationships***, or correlations between environmental variables (e.g., land cover) and detection or count data (Elith et al., 2006; MacKenzie et al., 2018). Agencies (i.e., federal, state and/or provincial wildlife management organizations) typically manage wildlife over broad spatial extents (Fig. S1) that are impractical to sample comprehensively, and thus available datasets are typically at resolutions too coarse to inform species-environment relationships at local scales (Bauder et al., 2020). However, many potential management actions (e.g., habitat manipulations, translocations) are local-scale phenomena, necessitating information about species distributions at fine resolutions to guide decisions (Moilanen et al., 2005; Wiens and Bachelet, 2010). *Therefore, wildlife managers should develop ways to use data that can be feasibly collected over broad spatial extents but can inform local-scale decisions.*

Historically, many agencies have used harvest data to monitor wildlife populations. Harvest data typically exist at broad extent (e.g., entire provinces) but at coarse resolution (counties or management units; Fig. S1). Agencies can use these data (in addition to age and sex ratios of harvested animals) in population reconstruction models to infer population size or trends within management units (Allen et al., 2018; Ryder, 2018). While this approach has been instrumental, harvest data have largely not been used to infer species-environment relationships

* Corresponding author.
E-mail address: nagilbert@wisc.edu (N.A. Gilbert).

https://doi.org/10.1016/j.biocon.2021.109147
Received 13 October 2020; Received in revised form 12 April 2021; Accepted 20 April 2021
Available online 9 May 2021

(and subsequently, fine-resolution occurrence or abundance patterns; but see Bauder et al., 2020). Knowledge of fine-resolution species distributions is important for targeted management actions such as resolving human-wildlife conflict. Therefore, managers need additional datasets and methods to quantify species-environment relationships, thus complementing harvest-based methods.

In recent years, citizen science has become a powerful datastream to quantify species-environment relationships (Dickinson et al., 2010). Recognizing the promise of citizen science, many agencies have launched citizen-science based monitoring programs (Lasky et al., 2021; Townsend et al., 2020). In particular, recent years have seen the emergence of ***jurisdictional observation networks (JONs)***, agency-coordinated efforts to collect ecological data at fine resolutions over broad spatial extents, often via passive sensors that are maintained by citizen scientists (Townsend et al., 2020). Passive sensors such as camera traps can effectively monitor diverse taxa while minimizing skill or effort biases associated with human observations (Burton et al., 2015; Wearn and Glover-Kapfer, 2019). However, JONs may not totally replace harvest-based wildlife monitoring. For example, JONs may rarely detect low-prevalence species; with few detections, fitting models and producing informative species-environment relationships is difficult. Ideally, managers should draw upon the strengths of both data sources to produce the best possible predictions of occurrence and abundance to guide decisions.

Harvest and camera-trap data are fundamentally observations of the same underlying ecological process: the distribution of animals in space. Reconciling differences between the datastreams within a single analysis is challenging (Pacifici et al., 2019), but ***integrated species distribution models*** (***iSDMs***; Isaac et al., 2020; Miller et al., 2019; Zipkin et al., 2019) provide a means to combine all available data to estimate species-environment relationships, thus informing species occurrence and abundance at fine resolution over broad spatial extents (Fig. 1A). Previous analyses have suggested that iSDMs generally reduce uncertainty in species-environment relationships, all within a single, streamlined approach (Fletcher et al., 2016; Isaac et al., 2020; Koshkina et al., 2017; Miller et al., 2019). However, the possibility of harvest data contributing to species distribution modeling has been largely overlooked (but see Bauder et al., 2020).

We applied iSDMs uniting JON camera-trap data and harvest records for six wildlife species representing a spectrum of prevalence in Wisconsin, USA (Fig. 1A–B). For comparison, we also developed camera-only and harvest-only SDMs (Fig. 1A). We hypothesized that iSDMs would produce more precise species-environment relationships than camera- and harvest-only models (Fig. 1C). In addition, we expected that iSDMs would capture spatial patterns of abundance intermediate to those predicted by individual data sources (Fig. 1D). Finally, we conducted a simulation study to evaluate the consequences of incomplete knowledge of harvest effort for estimates of abundance patterns and species-environment relationships.

2. Methods

2.1. Species

We focused on six wildlife species: wild turkey (*Meleagris gallopavo*; hereafter "turkey"), black bear (*Ursus americanus*; hereafter "bear"), river otter (*Lontra canadensis*; hereafter "otter"), fisher (*Pekania pennanti*), bobcat (*Lynx rufus*), and white-tailed deer (*Odocoileus virginianus*; hereafter "deer"). We chose these species because they are readily detected by cameras, their harvest is tracked by the Wisconsin Department of Natural Resources (WDNR), each is of management interest, and they represent a spectrum of prevalence (Fig. 1B).

2.2. Camera data

Our primary datastream was Snapshot Wisconsin, a JON operated by

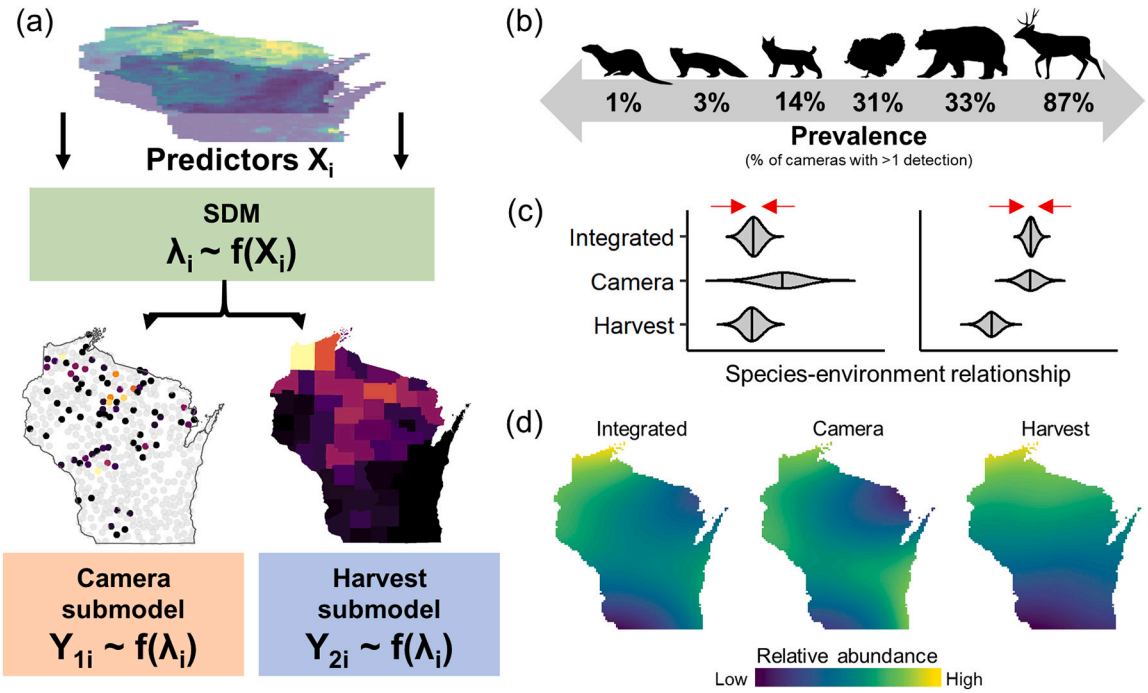

Fig. 1. (a) The iSDM framework with separate submodels for camera-trap data and harvest data (adapted from Miller et al., 2019); the camera- and harvest-only models contain submodels for only the camera and harvest data, respectively. (b) Focal species prevalence, defined as the percent of cameras that detected a species. From left to right, the silhouettes represent otter, fisher, bobcat, turkey, bear, and deer. (c) We predicted that integrated models would more precisely estimate species-environment relationships and that variance shrinking would be contingent upon species prevalence (left, low prevalence; right, high prevalence). (d) We predicted that harvest- and camera-only models would produce slightly different spatial patterns of abundance and that the patterns predicted by integrated models would be intermediate.

the WDNR (Fig. 2; Townsend et al., 2020). Snapshot Wisconsin has the dual goals of providing data to support wildlife management and increasing public engagement in wildlife science. The program relies on volunteers to host camera traps and classify images.

The WDNR solicits volunteers to host camera traps within US Public Land Survey System quarter-townships (spatial resolution, 4.8 × 4.8 km), which serve as sampling units for Snapshot Wisconsin. In an effort to maximize spatial coverage of the project, the WDNR prioritizes applicants from unoccupied cells. The WDNR provides each host with a Bushnell Trophy Cam (Overland Park, Kansas) with fixed settings such that the cameras record a 3-image sequence when triggered, with a 15-second gap between triggers. The hosts deploy their camera within their assigned quarter-township, typically on private land. They place their cameras along wildlife trails or water features at least 100 m from major roads or buildings. Hosts mount their camera 0.75–0.9 m from the ground and 3–4.5 m from the target, positioning the camera such that it aims the target at a diagonal angle and faces north to avoid false triggers from sunrise or sunset. Bait or lures are not used. Finally, hosts are instructed to clear vegetation between the camera and the target that may obstruct detection of animals. The hosts check their cameras every 1–3 months and upload the images to a web repository. Image classification takes three forms: 1) individual classifications by camera hosts, 2) consensus-based classification by volunteers on the Zooniverse crowdsourcing platform, 3) and expert classification of subsets of images to quantify accuracy of volunteer classifications (Anhalt-Depies et al., in prep). Since launching in 2016, Snapshot Wisconsin has generated >50 million photos from >2000 cameras.

We derived binary detection histories from the camera data to use in our analysis. First, we deleted photos if critical information (camera coordinates or date-time data) were missing or clearly wrong. We reviewed triggers classified as fisher or otter due to the relatively low classification accuracy for these species and updated the triggers' classification based upon review. Classification accuracy for the other species is sufficiently high (>98%; Anhalt-Depies in prep.; Clare et al., 2019) that we judged post hoc review unnecessary. Next, we defined the temporal extent of sampling and length of replicate sampling occasion for each species (Fig. 2). We focused on one year (2018) of data since our objective was to develop proof-of-concept models combining camera and harvest data. We defined a unique temporal extent for each species to restrict the camera data to times during which population closure was most likely, i.e., after reproduction but prior to the harvest season (Fig. 2). We defined the length of the replicate sampling occasions to be 7 days for the less-prevalent species and 1 day for the most common species (Fig. 2). We assigned NA values in the detection histories to cameras that were not active on particular sampling occasions. For each species, we filtered cameras that were active for at least two sampling occasions, though for turkey we filtered cameras that were active for all sampling occasions due to convergence issues in exploratory analyses. Number of camera locations for each species ranged from 524 (turkey) to 1439 (otter; Fig. 2). For each species, the median number of sampling occasions with active cameras was 8 (otter), 10 (fisher), 9 (bobcat), 31 (turkey), 9 (bear), and 15 (deer), respectively.

2.3. Harvest data

The WDNR regulates harvest within species-specific management zones (Fig. S1). However, the WDNR tracks annual harvest per county, which represent smaller areas than management zones for most species (Fig. S1). Therefore, we used the number of animals harvested within each county in 2018 as our second source of data (Fig. 2). Clearly, the number of animals harvested within a given county is a function of not only abundance but also of harvest effort. Therefore, we gleaned measures of harvest effort from the WDNR's 2018 harvest reports (WDNR, 2020) to be used as a bias term in the iSDMs (Fig. S2). Measures of harvest effort were based either on 1) the number of harvest authorizations per management unit or 2) metrics of harvest effort derived from WDNR hunter and trapper surveys. We were able to recover effort data at the county level for only two species (deer and bobcat); for the other

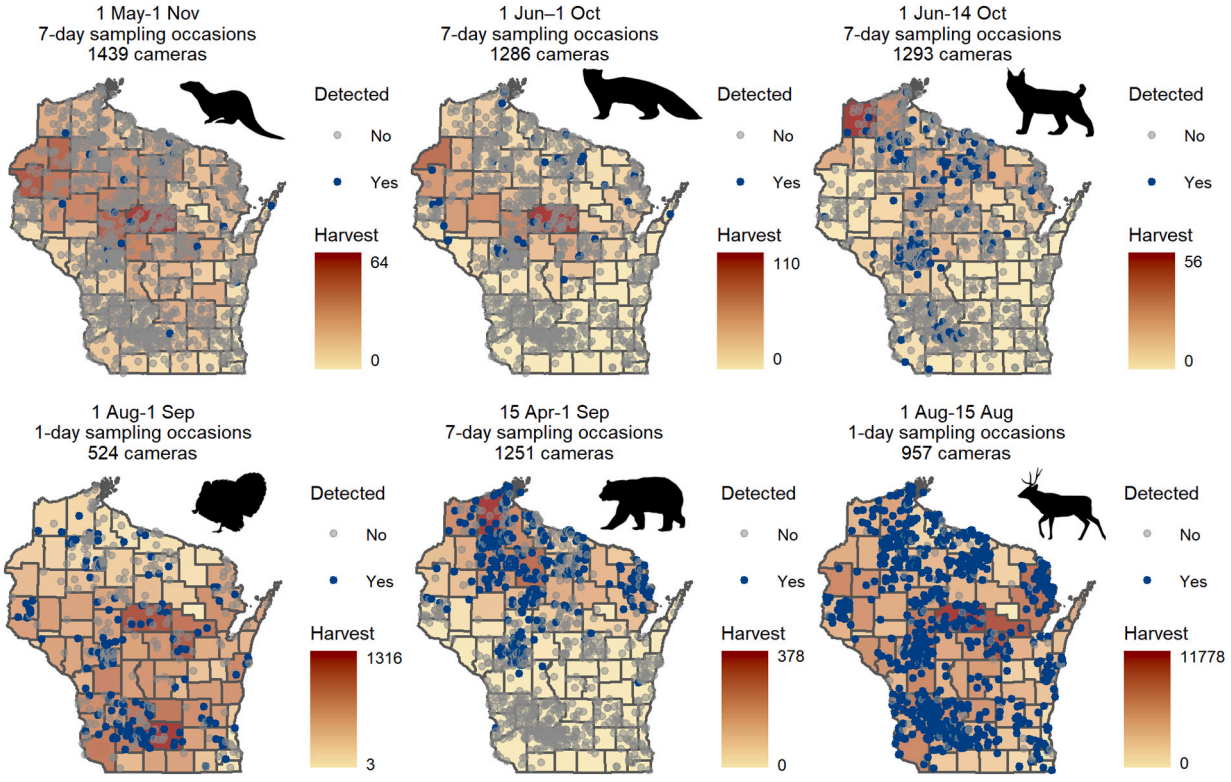

Fig. 2. Data used in analysis: county-level harvest (fill) and camera-trap detection records (points; translucent gray points represent cameras that never detected the species). The temporal extent, length of replicate sampling occasions, and number of locations for the camera data are shown above the map for each species.

species, we used information collected for larger management zones and assigned each zone's effort values to the counties whose centroids fell in that zone (Figs. S1, S2). We scaled the effort values to fall between 0 and 1. For more details on harvest effort data, please see Supplemental Information.

2.4. Modeling framework

2.4.1. Overview

Species distribution models create a statistical description of species occurrence and/or abundance, which are latent variables (i.e., cannot be directly observed). Therefore, SDMs use environmental predictors to characterize the distribution of interest and model uncertainty about observing the latent state via an observation submodel (Fig. 1A). Integrating multiple datastreams faces a fundamental challenge: different datastreams may arise from distinct sampling and observation processes (Fletcher et al., 2019). iSDMs address this challenge via datastream-specific observation submodels that inform a common ecological model (Fig. 1A).

Our two data sources represent detection-nondetection data (camera) and count data (harvest). To yoke these two distinct data currencies, we invoke a spatial point process as a unifying framework that generates both data types (Isaac et al., 2020; Miller et al., 2019). The expected abundance (λ) of the point process determines both whether a species occurs within some area as well as the true abundance (N) of the species within the same area. We consider space discrete and focus inference on expected abundance within grid cells (5 × 5 km resolution for 5 species and 8.5 × 8.5 km resolution for bears). Expected abundance λ is a shared parameter in both submodels (i.e., both data sources provide information about λ). Below, we use index i to reference cells within the prediction grid, index j to reference cameras, index k to reference sampling occasions, and index c to reference counties.

2.4.2. Model for latent state

We used a Royle-Nichols model (Royle and Nichols, 2003), which estimates abundance N via heterogeneity in detection-nondetection data. We modeled expected abundance λ as a function of environmental predictors and sampled the latent abundance state N:

$$log(\lambda_i) = \boldsymbol{\beta X}_i + \theta_i \tag{1}$$

$$N_i \sim Poisson(\lambda_i) \tag{2}$$

where λ_i is the expected abundance within the ith grid cell, $\boldsymbol{\beta}$ is a vector of regression coefficients, $\boldsymbol{X_i}$ is the design matrix of environmental predictors for the ith grid cell, and θ_i is a spatial random effect for the ith grid cell. We used weakly informative $\sim Normal(0, 2)$ priors—which are more robust to transformation than commonly used $\sim Normal(0, 100)$ priors—for the regression coefficients $\boldsymbol{\beta}$ (Banner et al., 2020; Hobbs and Hooten, 2015). We used a conditional autoregressive (CAR) prior for the spatial random effect θ_i, which acts as a cell-specific intercept by treating the random effect of the ith grid cell as conditional on the magnitude of neighbors' random effects as well as the strength of spatial dependence (Banerjee et al., 2015; Hoef et al., 2018). We used a $\sim Gamma(1, 1)$ hyperprior for the scalar precision of the CAR prior (Hoef et al., 2018).

For each species, we defined a parsimonious set of environmental predictors (i.e., $\boldsymbol{X_i}$ in Eq. (1)) that we hypothesized would drive its distribution; thus, different species had different predictors (Tables 1, S1). Because our goal was to compare results from iSDMs and individual-datastream SDMs (Fig. 1A), we defined a single global model rather than conducting multi-model inference. The covariates included percent canopy and impervious cover from the 2016 National Land Cover Database (Dewitz, 2019), mean annual temperature from WorldClim (Fick and Hijmans, 2017), edge density between forest and open land cover types from the 2018 MODIS land cover product (Friedl and Sulla-Menashe, 2019), and stream density from a shapefile of rivers and streams (ESRI, 2020; Fig. S3). Several other candidate predictors were omitted due to high (Pearson's $|r| > 0.7$) correlations with the other predictors (Dormann et al., 2013). We quantified mean values of the predictors within 5 × 5 km (5 species) and 8.5 × 8.5 km (bear) grid cells to roughly match the space use of each species (Schank et al., 2019; Supplemental information).

Table 1
Variables used to predict expected abundance (Environmental predictors) and per-individual detection probability (Detection predictors) for each species. Please see Table S1 for a detailed justification of the environmental predictors used.

Species	Environmental predictors	Detection predictors
Otter	Canopy cover, impervious cover, stream density	Local canopy, date, date^2, camera height, target distance
Fisher	Canopy cover, impervious cover	Local canopy, date, date^2, camera height, target distance
Bobcat	Canopy cover, impervious cover	Local canopy, date, date^2, camera height, target distance
Turkey	Mean annual temperature, impervious cover, forest-open edge	Local canopy, camera height, target distance
Bear	Canopy cover, impervious cover	Local canopy, date, date^2, camera height, target distance
Deer	Mean annual temperature, impervious cover, forest-open edge	Local canopy, date, camera height, target distance

2.4.3. Camera submodel

Observational submodels are conditional on the latent state. In the case of the Royle-Nichols model, the submodel describes the probability of detecting an animal, *given abundance of the species at the location* (Royle and Nichols, 2003). We allowed detection probability to vary by camera and sampling occasion via covariates and random effects.

$$Y_{1jk} \sim Bernoulli(p_{jk}) \tag{3}$$

$$p_{jk} = 1 - (1 - r_{jk})^{N_j} \tag{4}$$

$$logit(r_{jk}) = \boldsymbol{\alpha X_{jk}} + \varepsilon_{jk} \tag{5}$$

where Y_{1jk} is a binary indicator of whether the focal species was detected at the jth camera during the kth sampling occasion, p_{jk} is the per-camera detection probability at the jth camera during the kth sampling occasion, N_j is abundance within the grid cell containing the jth camera, and r_{jk} is per-individual detection probability at the jth camera during the kth sampling occasion. In Eq. (5), $\boldsymbol{\alpha}$ is a coefficient vector, $\boldsymbol{X_{jk}}$ is the corresponding design matrix of detection predictors, and ε_{jk} is a camera- and sampling occasion-level random effect. We used percent canopy cover within the 30 × 30 m grid cell containing each camera (reasoning that forest structure may correlate with animal detectability), ordinal date, camera height, and distance to the targeted trail as detection predictors (Table 1, Supplemental information). We used ~Logistic(0, 1) priors for $\boldsymbol{\alpha}$ (Banner et al., 2020) and a ~Normal(0, σ) prior for ε_{jk}, where σ is a hyperprior modeled with a ~Gamma(1, 2) distribution.

2.4.4. Harvest submodel

The harvest data exists at a coarser spatial resolution than the camera data and environmental predictors (Pacifici et al., 2019). Such a misalignment of spatial resolution between data sources can lead to severe biases if not addressed (Banerjee et al., 2015; Pacifici et al., 2019). Therefore, we defined county-level expected abundance to be a linear function of the sum of fine-resolution expected abundances within a given county; that is, we induce a formal statistical change-of-support to reconcile the spatial misalignment between the point-level camera observations and the areal harvest counts to make inference at the grid cell resolution described above (Pacifici et al., 2019).

$$log(\lambda County_c) = \gamma_0 + \gamma_1 log\left(\sum_{i=c1}^{n=c2} \lambda_i\right) \quad (6)$$

$$Harvest_c \sim Poisson(effort_c * \lambda County_c) \quad (7)$$

where $\lambda County_c$ is expected abundance for the cth county, γ_0 and γ_1 are the intercept and slope, respectively, of the equation scaling fine-resolution expected abundance to county-resolution expected abundance, and c1 and c2 index the first and last cells, respectively, to fall within county c. We used $\sim Normal(0, 2)$ priors for γ_0 and γ_1. Importantly, this scaling equation implies that county-level abundance need not be a simple sum of grid-level abundances, thus accommodating issues such as different sampling exposure of grid-level and county-level subpopulations or suboptimal grid resolution selection. Finally, $Harvest_c$ and $effort_c$ are the harvest count and effort data for the cth county.

2.4.5. Model evaluation

We compared results for three models: an integrated model with submodels for both data sources (*integrated*), a model with a camera submodel only (*camera-only*), and a model with a harvest submodel only (*harvest-only*). Discriminating among these models is a challenge, since model-ranking methods (e.g., AIC) are not appropriate for use with models that contain different sets of observations (Isaac et al., 2020). Moreover, because the species' true distributions are unknown, we cannot evaluate which model provides more accurate results. Consequently, we compared estimates of species-environment relationships and expected abundance from the three models and conducted a simulation study (see next section) to evaluate possible biases.

We compared the precision of species-environment relationships (i.e., the coefficient vector $\boldsymbol{\beta}$ from Eq. (1)) estimated by the three models (Fig. 1B). The variance of a coefficient represents uncertainty about the relationship between a predictor and expected abundance. While a coefficient's variance is not indicative of model fit or performance per se, we reasoned that practitioners want models that reduce uncertainty in species-environment relationships as much as possible (Milner-Gulland and Shea, 2017; Nicol et al., 2019; but see Graves et al., 2012).

In addition, we compared patterns of expected abundance (i.e., λ_i in Eq. (1)) and occurrence probability ψ_i (converted from expected abundance λ_i) predicted by the three models to evaluate how the models might provide different information in a management context. For both expected abundance and occurrence, we computed Pearson's correlation coefficient r for all cells across the entire state. For expected abundance, we compared areas that each model predicted to have the lowest and highest expected abundance, reasoning that areas of rarity and high abundance are both of management significance. To do so, for each model, we selected grid cells within the 90th and 10th percentiles for λ_i. We then mapped these cells to evaluate levels of agreement between models about areas predicted to have the lowest and highest expected abundance. We define "agreement" as the proportion of overlapping 10th or 90th percentile cells between multiple models.

We ran all models in the R package NIMBLE 0.8.0 (de Valpine et al., 2017; R Core Team, 2019). We ran three Markov Chain Monte Carlo (MCMC) chains and assessed convergence via visual inspection of traceplots and the Gelman-Rubin diagnostic $\widehat{R}$ (considering parameters with $\widehat{R} \leq 1.1$ to be converged; Brooks and Gelman, 1998). We ran chains until they converged or reached 100,000 iterations, at which point we declared the model unconverged.

2.5. Simulation study

The goal of the simulation study was to evaluate the consequences of incomplete knowledge of harvest effort for estimates of expected abundance λ_i and species-environment relationships. For a low- and a high-prevalence "pseudospecies", we ran a camera-only, a harvest-only, and two integrated models with mediocre and quality effort data, respectively (thus for a total of 8 simulation scenarios, each of which we replicated 100 times). We created a grid of 1296 fine-resolution cells nested within 36 coarse-resolution cells (i.e., each coarse cell contained 36 fine cells; Fig. 3). This roughly corresponds to the resolution misalignment in our empirical data; for the bear model, each county contained an average of 30 cells, and for the other species, each county contained an average of 85 cells. For both pseudospecies, we generated fine-cell expected abundance λ_i as a function of the grid's x- and y-coordinates, as follows:

$$log(\lambda_i) = \beta_0 + \beta_1 x_i + \beta_2 y_i + \varepsilon_i \quad (8)$$

where β_0 is the average expected abundance, fixed to 0 for the low-prevalence pseudospecies and 1 for the high-prevalence pseudospecies. β_1 and β_2 are species-environment relationships; we fixed the values of these coefficients at -0.5 and 1.25, respectively, which roughly matches the magnitude of the species-environment relationships estimated in our empirical application. Finally, x_i and y_i are the x- and y-coordinates (minima and maxima of -1 and 1, respectively) of the cell's center, and ε_i is cell-specific noise drawn from a $\sim$Normal(0, 0.1) distribution. We intended the low-prevalence pseudospecies (median $\lambda_i = 0.98$, IQR 0.53–1.87) to represent the less prevalent species in our dataset (e.g., fisher; Fig. 1) and the high-prevalence pseudospecies (median $\lambda_i = 2.66$, IQR 1.45–5.10) to represent the more prevalent species in our dataset (e.g., turkey; Fig. 1). We sampled abundance N_i from a Poisson distribution (Fig. 3a). Finally, we randomly selected 15% of the fine cells to survey and generated 15 replicate surveys by sampling a binomial distribution, fixing per-individual detection probability at 0.1 (Fig. 3b). In our empirical data, the average percentage of fine cells surveyed (across species) was 14% and the average number of replicate surveys (across species) was 13.67. Additionally, exploratory analyses suggested that per-individual detection probabilities for most of the species considered were comparably low.

We calculated coarse cell abundance N_c as the sum of fine-cell abundances N_i nested within each coarse cell (Fig. 3c). We assigned each coarse cell a random per-individual harvest probability between 0 and 0.5 (Fig. 3d) and sampled harvest counts from a binomial distribution (Fig. 3e). The varying per-individual harvest probability represents variable harvest effort (and consequently, varying proportions of the coarse-cell population harvested) in different counties. For the integrated models, we evaluated "mediocre" and "quality" effort scenarios in which county-level effort was modestly ($r = 0.46$) and strongly ($r = 0.94$) correlated with county-level harvest probability (Fig. 3f). For the harvest-only model, we included the quality-level effort data. All models included each cell's x- and y-coordinates as predictors as well as an intercept. We ran all models for 20,000 MCMC iterations in NIMBLE (de Valpine et al., 2017) and discarded all but the final 1000 iterations as burn-in. We evaluated model performance in all scenarios by 1) calculating the relative bias of expected abundance λ_i, 2) calculating the standard deviation of estimated expected abundance λ_i, 3) and assessing accuracy and precision of the species-environment relationships in Eq. (8). Please see Supplemental information for code to run the simulation.

3. Results

3.1. Species-environment relationships

We estimated 15 species-environment relationships (2–3 predictors for each of 6 species; Table 1). Harvest-only models failed to converge. Thus, we only report results from integrated and camera-only models. Integrated models produced more precise species-environment relationships for 8 (53%) of the relationships (Fig. 4). The signs of relationships estimated by the two models for a species were always the same (Fig. 4). However, in three cases (stream density for otter and edge density for turkey and deer), the integrated model estimated a relationship that did not overlap zero, while the camera-only model

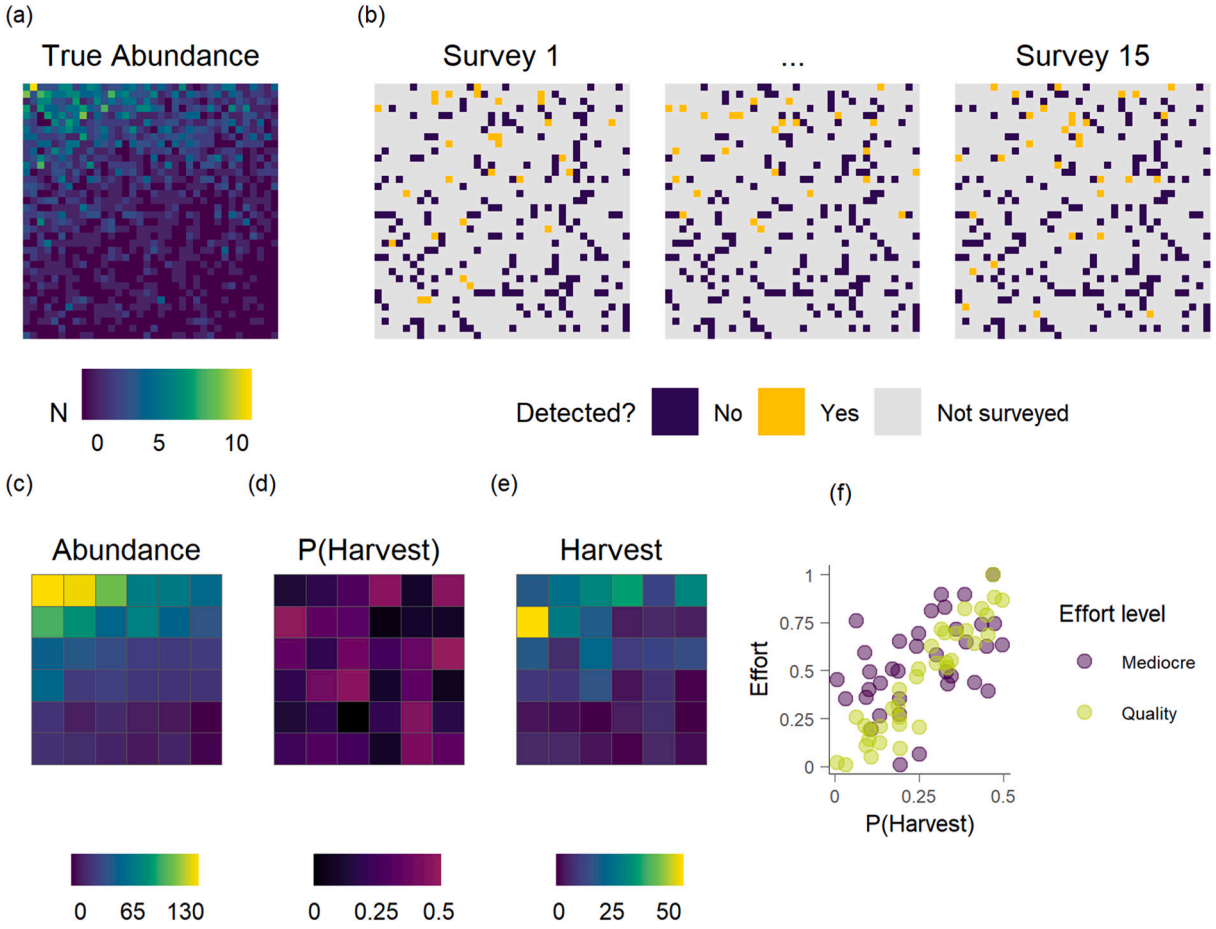

Fig. 3. Setup of simulation study to evaluate the effects of incomplete knowledge of harvest effort. In (a), fine-resolution abundance is highest in the upper left part of the landscape; (b) shows 3 of the 15 replicate fine-resolution surveys in which 15% of the cells were surveyed to produce detection-nondetection data. Each coarse-resolution cell contained 36 fine cells (c), and probability of harvest varied among the coarse cells (d) such that the harvest counts (e) were imperfect representations of underlying coarse-resolution abundance. Finally, we evaluated integrated models with varying quality of effort data (f).

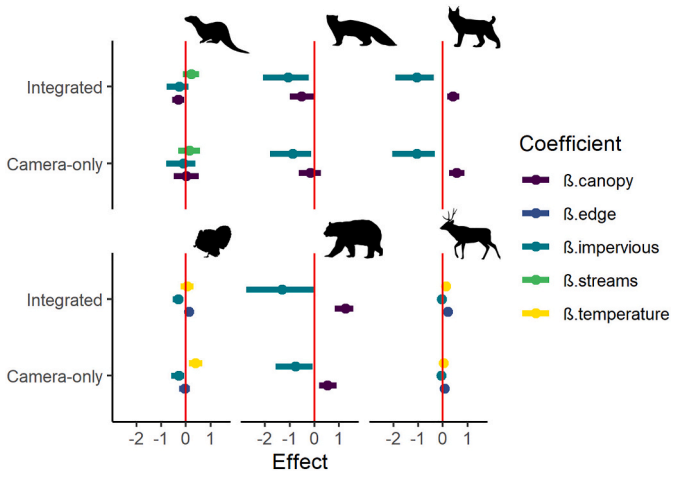

Fig. 4. Posterior distributions of species-environment relationships. Harvest-only results omitted because models did not converge. The points and bars represent the coefficients' posterior means and 95% credible intervals, respectively. The dashed red lines represent no relationship between the predictor and expected abundance. (For interpretation of the references to colour in this figure legend, the reader is referred to the web version of this article.)

estimated a relationship that did overlap zero (Fig. 4). Conversely, in two cases (percent canopy for bear and mean annual temperature for turkey), the camera-only model estimated a relationship that did not overlap zero, whereas the integrated model produced a relationship that overlapped zero (Fig. 4).

Regarding species prevalence and species-environment relationships, trends predicted in Fig. 1B partly emerged. As predicted, the most precise relationships were estimated for deer, the most prevalent species (Figs. 1B, 4). However, the least precise relationships were *not* for the least prevalent species (e.g., otter coefficients were more precise than bear coefficients).

3.2. Patterns of expected abundance and occurrence

Integrated and camera-only models generally did not identify the same abundance hotspots. Bobcat and turkey showed the highest (40%) and lowest (3%) levels of agreement, respectively, about high-abundance areas (Fig. 5). In contrast, four species showed higher levels of agreement about abundance cold spots, with otter and deer being the exceptions (Fig. S4). Bear showed the highest agreement about low-abundance areas (82%), while otter showed the lowest (10%; Fig. S4). The strongest correlation between expected abundances predicted by the two models was for bobcat (0.80) and weakest for otter (0.12; Table S2). With expected abundance translated to occurrence, the integrated and camera-only models predicted similar spatial patterns of occurrence for most species (Fig. 6). Correlations between occurrence predicted by the two models was slightly stronger than the abundance

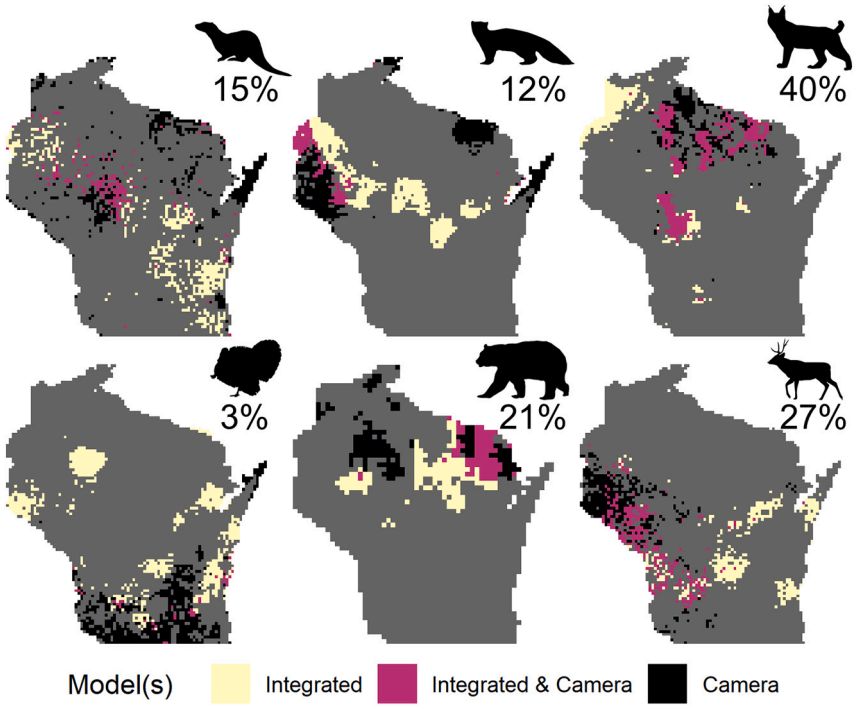

Fig. 5. Regions of highest expected abundance (90th percentile) as predicted by the camera-only and integrated models. Areas where the two models agree are shown in purple; the percent agreement is displayed under the silhouette of each species. (For interpretation of the references to colour in this figure legend, the reader is referred to the web version of this article.)

correlations except for deer (Fig. 6, Table S2). Notably, while bear expected abundance predicted by the two models was only modestly correlated (0.58), bear occurrence correlation between the two models was strong (0.87; Fig. 6).

3.3. Simulation study

The camera-only and integrated models produced estimates of expected abundance λ_i with limited bias (<5%); the harvest-only model produced highly biased results (Fig. 7). For the high-abundance pseudospecies, the "quality effort" integrated model produced less biased (−1%) estimates than the "mediocre effort" integrated model (−5%; Fig. 7). In addition, the integrated models produced more precise estimates than the camera-only model, and the "quality effort" scenario produced more precise estimates than the "mediocre effort" scenario (Fig. 7).

The camera-only and integrated models identified the true species-environment relationships; the harvest-only estimates were extremely imprecise and overlapped zero (Fig. S5). In all but one case (β_2 from the integrated model with mediocre effort for the high-prevalence pseudospecies), the integrated models produced more precise estimates of species-environment relationships than the camera-only model (Fig. S5). The two effort scenarios in integrated models produced species-environment relationships with similar levels of precision (Fig. S5).

4. Discussion

Integrated models produced more precise species-environment relationships than camera-only models in a narrow majority of cases, and harvest-only models failed to converge (Fig. 4). The fact that harvest-only models did not converge suggests that harvest data alone cannot be used to inform species distributions at fine resolution and in turn guide local-scale management efforts (Bauder et al., 2020). Simulations corroborated this idea, as the harvest-only model produced extremely biased and imprecise estimates of expected abundance and species-environment relationships (Figs. 7, S5). Taken together, these results suggest that harvest records should be supplemented with fine-resolution data to inform local-scale management. Cameras represent a good supplementary datastream because they provide occurrence data at an exact point in space, which facilitates the identification of species-environment relationships.

Our results suggest that camera networks can benefit from the integration of harvest data, particularly if high-quality harvest effort data is available. Assuming quality effort data is available, the information added by harvest can generate more precise species-environment relationships; for rare or difficult-to-detect species, the added information may make all the difference between an informative species-environment relationship and a relationship too imprecise to support management decisions. We note that a JON on the scale of Snapshot Wisconsin is not required to redeem harvest records for fine-resolution inference; for example, even 30–100 strategically-placed cameras paired with harvest data would likely permit identification of species-environment relationships (e.g., Kays et al., 2020; Simmonds et al., 2020). Emerging fine-resolution datastreams and iSDMs provide managers with the option to co-opt existing, coarse-resolution datasets to make fine-resolution predictions of species distributions. These predictions, in turn, can be used to guide local-scale management actions such as identifying areas for human-wildlife conflict resolution.

We found low agreement in areas predicted to be abundance hotspots by the integrated and camera-only models. While it is difficult to judge which model better predicts the latent species distribution, the fact that two models show low agreement is still informative for decision-makers. Because agencies must make management decisions with incomplete information, managers should draw upon multiple sources of data to navigate decisions. For example, agencies occasionally reconfigure management zones based on perceived abundance. Low agreement about high-abundance regions between models might reduce managers' confidence in delineating new management zones, whereas high agreement would provide robust justification for such management

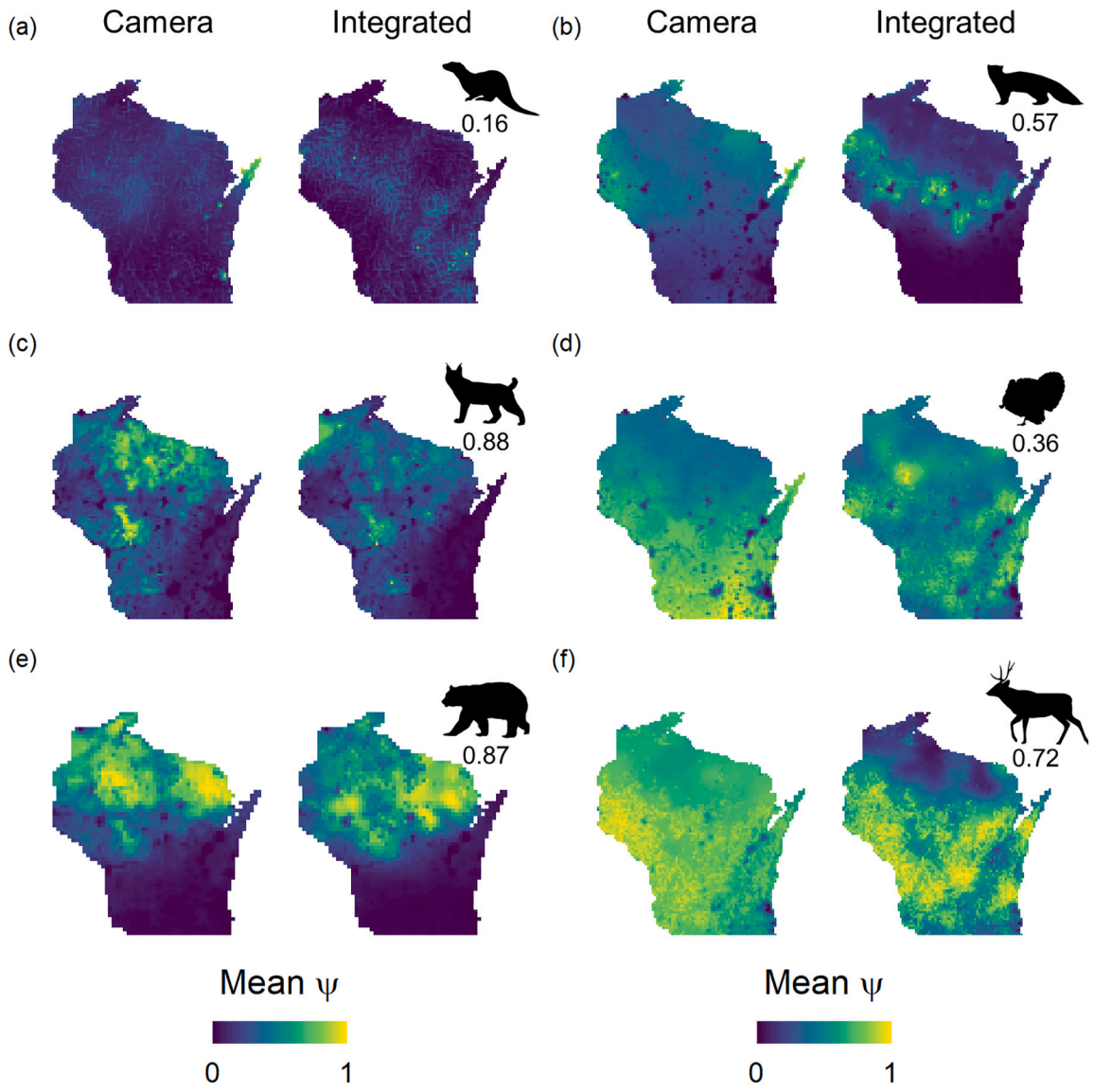

Fig. 6. Occurrence probability (mean) for the six focal species from integrated and camera-only models (harvest-only results omitted due to convergence issues). Occurrence probabilities are scaled to have minima and maxima of 0 and 1, respectively, to facilitate comparisons. The numbers beneath the species silhouettes are the correlations between occurrence values predicted by the two models.

decisions. Managers might target low-agreement regions with fine-resolution sampling to help resolve uncertainty in estimates of species distributions. In other words, managers can use integrated and single-datastream analyses to cross-check each other when facing management decisions.

4.1. Recommendations for wildlife management agencies

4.1.1. Enhance effort reporting

As demonstrated by our simulation study, high-quality effort data can help improve the precision (and in some cases, accuracy) of estimates of species-environment relationships and expected abundance (Pacifici et al., 2019). Our simulations suggest that poor effort information can lead to particularly misleading results for high-abundance species (Fig. 7). In our empirical application, we had harvest effort data at the scale of harvest records (the county) for only two species, making it difficult to separate variation in the harvest counts that arise due to the ecological process (the species' distribution) versus the observational process (hunting effort). We suggest that agencies expand programs to track harvest effort data. While implementing mandatory effort reporting would be logistically challenging and potentially face pushback from hunters (Kilpatrick et al., 2005; Schmidt and Chapman, 2014), such information would increase the value of harvest records as a form of distribution data.

4.1.2. Track harvest at finer spatial resolution

Agencies commonly monitor wildlife species within taxon-specific jurisdictional units that cover vast areas (Fig. S1). While it is desirable to tailor unit delineations to match the system of interest, we suggest that tracking harvest at finer resolution would increase the value of these data for distribution modeling (Bauder et al., 2020). One possible solution would be to adopt a single system of finer-resolution jurisdictional units. In particular, effort reporting would be simplified for hunters and trappers if these records were collected within units that are readily recognized by the public (e.g., counties or townships), rather than species-specific management units. Implementing such changes would require considerable agency resources and likely be difficult given the idiosyncratic governance structure for each species, but we suggest it could enhance the quality of harvest records.

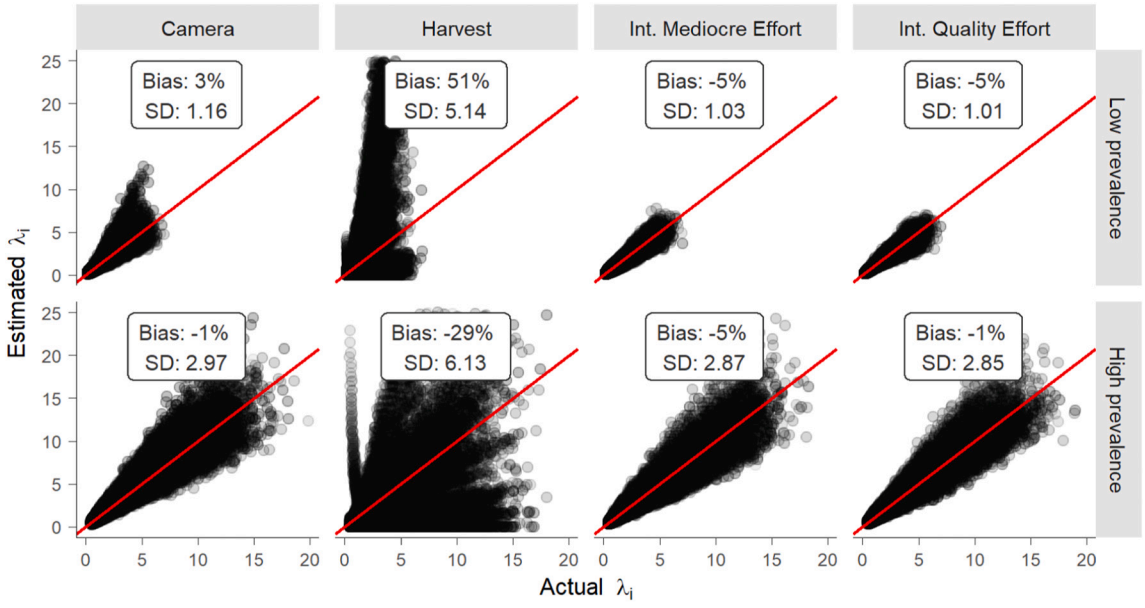

Fig. 7. Bias and precision of estimates of expected abundance λ from 8 simulation scenarios. The red lines show the 1:1 relationship between estimated and actual expected abundance, "Bias" is the relative bias of estimated expected abundance, and SD is the standard deviation of estimated expected abundance. Rows represent a low- and high-prevalence "pseudospecies"; the columns represent camera-only, harvest-only, and integrated models with mediocre and quality effort information, respectively. (For interpretation of the references to colour in this figure legend, the reader is referred to the web version of this article.)

4.1.3. Expand taxonomic resolution

One of the appealing aspects of cameras is that they represent a means to conduct broad-spectrum monitoring of multiple species simultaneously (Burton et al., 2015). In contrast, agencies often do not track harvest of all game species. For example, in Wisconsin, harvest is regulated but not tracked at resolution finer than the state level for a number of species, including snowshoe hare (*Lepatius americanus*) and ruffed grouse (*Bonasa umbellus*). Harvest records for such taxa could enhance camera-based efforts to monitor these species (Townsend et al., 2020). While expanding harvest record-keeping would be a logistical challenge, we emphasize that it would provide information that could improve predictions of species distributions, which is an appealing prospect because the aforementioned species are declining in the region and considered vulnerable to climate change (Shipley et al., 2019; Wilson et al., 2019).

4.2. Conclusion

We highlight the potential of integrating emerging datastreams with pre-existing forms of ecological data. Camera traps and harvest records are not the only data types that fit within this framework; for example, acoustic monitoring datastreams from JONs could be combined with coarser-resolution bird atlas data. In addition, the iSDM framework is flexible and can accommodate alternate submodels for cases in which researchers collect fine-resolution count (rather than detection-nondetection) data. Our simulation study underscores the need for quality information on effort for the coarser-resolution data. Our application demonstrates that integrated models can provide more precise species-environment relationships and may identify different spatial patterns of occurrence and abundance from individual-datastream models. We highlight that multiple sources of data can be used to cross-check each other and bolster management decisions. We anticipate that integrated approaches to species distribution modeling will continue to grow and encourage practitioners to tailor existing forms of data collection to accommodate emerging datastreams from observation networks.

CRediT authorship contribution statement

NAG and BZ conceived the study. NAG, BSP, and JLS compiled and analyzed the data with input from BZ. NAG wrote the manuscript, and all authors contributed critically to the drafts and gave final approval for publication.

Declaration of competing interest

The authors declare that they have no known competing financial interests or personal relationships that could have appeared to influence the work reported in this paper.

Acknowledgements

We thank the thousands of Snapshot Wisconsin volunteers who collected and processed data, including trail camera hosts and Zooniverse photo classifiers. We also thank the hunters, trappers, and WDNR wildlife management staff who collected and provided harvest data for the analysis. This publication uses data generated via the Zooniverse.org platform, funded in part by a grant from the Alfred P. Sloan Foundation and a Global Impact Award from Google. Support was provided by NASA Ecological Forecasting #NNX14AC36G to PAT, BZ and TVD, and NASA #NNX16AO61H to JC. This publication was, in part, jointly developed and funded by the Wisconsin Department of Natural Resources and the UW College of Agriculture and Life Sciences as USFWS Federal Aid in Wildlife Restoration Project. We are grateful for additional support from the Department of Forest and Wildlife Ecology at UW-Madison. Finally, we thank Remington Moll and an anonymous reviewer whose comments improved the manuscript.

Data availability statement

Data and code to fit models are posted in a public GitHub repository (https://github.com/n-a-gilbert/isdm_examples) and on Figshare (https://doi.org/10.6084/m9.figshare.c.5414523).

Appendix A. Supplementary data

Supplementary data to this article can be found online at https://doi.org/10.1016/j.biocon.2021.109147.

References

Allen, M.L., Norton, A.S., Stauffer, G., Roberts, N.M., Luo, Y., Li, Q., MacFarland, D., Deelen, T.R.V., 2018. A Bayesian state-space model using age-at-harvest data for estimating the population of black bears (Ursus americanus) in Wisconsin. Sci. Rep. 8, 12440. https://doi.org/10.1038/s41598-018-30988-4.

Banerjee, S., Carlin, B., Gelfand, A., 2015. Hierarchical Modeling and Analysis for Spatial Data, 2nd ed. CRC Press, Boca Raton, FL.

Banner, K.M., Irvine, K.M., Rodhouse, T., 2020. The use of Bayesian priors in ecology: the good, the bad, and the not great. Methods Ecol. Evol. 11, 882–889. https://doi.org/10.1111/2041-210X.13407.

Bauder, J.M., Cervantes, A.M., Avrin, A.C., Whipple, L.S., Farmer, M.J., Miller, C.A., Benson, T.J., Stodola, K.W., Allen, M.L., 2020. Mismatched spatial scales can limit the utility of citizen science data for estimating wildlife-habitat relationships. Ecol. Res. 1–10. https://doi.org/10.1111/1440-1703.12173.

Brooks, S.P., Gelman, A., 1998. General methods for monitoring convergence of iterative simulations. J. Comput. Graph. Stat. 7, 434–455. https://doi.org/10.1080/10618600.1998.10474787.

Burton, A.C., Neilson, E., Moreira, D., Ladle, A., Steenweg, R., Fisher, J.T., Bayne, E., Boutin, S., 2015. Wildlife camera trapping: a review and recommendations for linking surveys to ecological processes. J. Appl. Ecol. 52, 675–685. https://doi.org/10.1111/1365-2664.12432.

Clare, J.D.J., Townsend, P.A., Anhalt-Depies, C., Locke, C., Stenglein, J.L., Frett, S., Martin, K.J., Singh, A., Deelen, T.R.V., Zuckerberg, B., 2019. Making inference with messy (citizen science) data: when are data accurate enough and how can they be improved? Ecol. Appl. 29, e01849 https://doi.org/10.1002/eap.1849.

de Valpine, P., Turek, D., Paciorek, C.J., Anderson-Bergman, C., Lang, D.T., Bodik, R., 2017. Programming with models: writing statistical algorithms for general model structures with NIMBLE. J. Comput. Graph. Stat. 26, 403–413. https://doi.org/10.1080/10618600.2016.1172487.

Dewitz, J., 2019. National Land Cover Database (NLCD) 2016 products: U.S. Geological Survey data release.

Dickinson, J.L., Zuckerberg, B., Bonter, D.N., 2010. Citizen science as an ecological research tool: challenges and benefits. Annu. Rev. Ecol. Evol. Syst. 41, 149–172. https://doi.org/10.1146/annurev-ecolsys-102209-144636.

Dormann, C.F., Elith, J., Bacher, S., Buchmann, C., Carl, G., Carré, G., Marquéz, J.R.G., Gruber, B., Lafourcade, B., Leitão, P.J., Münkemüller, T., McClean, C., Osborne, P.E., Reineking, B., Schröder, B., Skidmore, A.K., Zurell, D., Lautenbach, S., 2013. Collinearity: a review of methods to deal with it and a simulation study evaluating their performance. Ecography 36, 27–46. https://doi.org/10.1111/j.1600-0587.2012.07348.x.

Elith, J., Graham, C.H., Anderson, R.P., Dudik, M., Ferrier, S., Guisan, A., Hijmans, R.J., Huettmann, F., Leathwick, J.R., Lehmann, A., Li, J., Lohmann, L.G., Loiselle, B.A., Manion, G., Moritz, C., Nakamura, M., Nakazawa, Y., Overton, J.M., Peterson, A.T., Phillips, S.J., Richardson, K., Scachetti-Pereira, R., Schapire, R.E., Soberon, J., Williams, S., Wisz, M.S., Zimmermann, N.E., 2006. Novel methods improve prediction of species' distributions from occurrence data. Ecography 29, 129–151. https://doi.org/10.1111/j.2006.0906-7590.04596.x.

ESRI, 2020. USA rivers and streams.

Fick, S.E., Hijmans, R.J., 2017. WorldClim 2: new 1-km spatial resolution climate surfaces for global land areas. Int. J. Climatol. 37, 4302–4315. https://doi.org/10.1002/joc.5086.

Fletcher, R.J., McCleery, R.A., Greene, D.U., Tye, C.A., 2016. Integrated models that unite local and regional data reveal larger-scale environmental relationships and improve predictions of species distributions. Landsc. Ecol. 31, 1369–1382. https://doi.org/10.1007/s10980-015-0327-9.

Fletcher, R.J., Hefley, T.J., Robertson, E.P., Zuckerberg, B., McCleery, R.A., Dorazio, R. M., 2019. A practical guide for combining data to model species distributions. Ecology 100, e02710. https://doi.org/10.1002/ecy.2710.

Friedl, M., Sulla-Menashe, D., 2019. MCD12Q1 MODIS/Terra+Aqua land cover type yearly L3 global 500m SIN grid V006. In: NASA EOSDIS Land Processes DAAC.

Graves, T.A., Royle, J.A., Kendall, K.C., Beier, P., Stetz, J.B., Macleod, A.C., 2012. Balancing precision and risk: should multiple detection methods be analyzed separately in N-mixture models? PLoS One 7, e49410. https://doi.org/10.1371/journal.pone.0049410.

Hobbs, N.T., Hooten, M., 2015. Bayesian Models: A Statistical Primer for Ecologists. Princeton University Press, Princeton, NJ.

Hoef, J.M.V., Peterson, E.E., Hooten, M.B., Hanks, E.M., Fortin, M.-J., 2018. Spatial autoregressive models for statistical inference from ecological data. Ecol. Monogr. 88, 36–59. https://doi.org/10.1002/ecm.1283.

Isaac, N.J.B., Jarzyna, M.A., Keil, P., Dambly, L.I., Boersch-Supan, P.H., Browning, E., Freeman, S.N., Golding, N., Guillera-Arroita, G., Henrys, P.A., Jarvis, S., Lahoz-Monfort, J., Pagel, J., Pescott, O.L., Schmucki, R., Simmonds, E.G., O'Hara, R.B., 2020. Data integration for large-scale models of species distributions. Trends Ecol. Evol. 35, 56–67. https://doi.org/10.1016/j.tree.2019.08.006.

Kays, R., Arbogast, B.S., Baker-Whatton, M., Beirne, C., Boone, H.M., Bowler, M., Burneo, S.F., Cove, M.V., Ding, P., Espinosa, S., Gonçalves, A.L.S., Hansen, C.P., Jansen, P.A., Kolowski, J.M., Knowles, T.W., Lima, M.G.M., Millspaugh, J., McShea, W.J., Pacifici, K., Parsons, A.W., Pease, B.S., Rovero, F., Santos, F., Schuttler, S.G., Sheil, D., Si, X., Snider, M., Spironello, W.R., 2020. An empirical evaluation of camera trap study design: how many, how long and when? Methods Ecol. Evol. 11, 700–713. https://doi.org/10.1111/2041-210X.13370.

Kilpatrick, H.J., LaBonte, A.M., Barclay, J.S., 2005. Factors affecting harvest-reporting rates for white-tailed deer. Wildl. Soc. Bull. 33, 974–980. https://doi.org/10.2193/0091-7648(2005)33[974:FAHRFW]2.0.CO;2.

Koshkina, V., Wang, Y., Gordon, A., Dorazio, R.M., White, M., Stone, L., 2017. Integrated species distribution models: combining presence-background data and site-occupancy data with imperfect detection. Methods Ecol. Evol. 8, 420–430. https://doi.org/10.1111/2041-210X.12738.

Lasky, M., Parsons, A., Schuttler, S., Mash, A., Larson, L., Norton, B., Pease, B., Boone, H., Gatens, L., Kays, R., 2021. Candid critters: challenges and solutions in a large-scale citizen science camera trap project. Citizen Sci. Theory Pract. 6, 4. https://doi.org/10.5334/cstp.343.

MacKenzie, Nichols, J., Royle, J., Pollock, K., Bailey, L., Hines, J., 2018. Occupancy Estimation and Modeling: Inferring Patterns and Dynamics of Species Occurrence, 2nd ed. Academic Press, London.

Miller, D.A.W., Pacifici, K., Sanderlin, J.S., Reich, B.J., 2019. The recent past and promising future for data integration methods to estimate species' distributions. Methods Ecol. Evol. 10, 22–37. https://doi.org/10.1111/2041-210X.13110.

Milner-Gulland, E.J., Shea, K., 2017. Embracing uncertainty in applied ecology. J. Appl. Ecol. 54, 2063–2068. https://doi.org/10.1111/1365-2664.12887.

Moilanen, A., Franco, A.M.A., Early, R.I., Fox, R., Wintle, B., Thomas, C.D., 2005. Prioritizing multiple-use landscapes for conservation: methods for large multi-species planning problems. Proc. R. Soc. B Biol. Sci. 272, 1885–1891. https://doi.org/10.1098/rspb.2005.3164.

Nicol, S., Brazill-Boast, J., Gorrod, E., McSorley, A., Peyrard, N., Chadès, I., 2019. Quantifying the impact of uncertainty on threat management for biodiversity. Nat. Commun. 10, 3570. https://doi.org/10.1038/s41467-019-11404-5.

Pacifici, K., Reich, B.J., Miller, D.A.W., Pease, B.S., 2019. Resolving misaligned spatial data with integrated species distribution models. Ecology 100, e02709. https://doi.org/10.1002/ecy.2709.

R Core Team, 2019. R: A Language and Environment for Statistical Computing. R Foundation for Statistical Computing, Vienna, Austria.

Royle, J.A., Nichols, J.D., 2003. Estimating abundance from repeated presence–absence data or point counts. Ecology 84, 777–790. https://doi.org/10.1890/0012-9658(2003)084[0777:EAFRPA]2.0.CO;2.

Ryder, T. (Ed.), 2018. State Wildlife Management and Conservation, 1st ed. Johns Hopkins University Press, Baltimore MD.

Schank, C.J., Cove, M.V., Kelly, M.J., Nielsen, C.K., O'Farrill, G., Meyer, N., Jordan, C.A., González-Maya, J.F., Lizcano, D.J., Moreno, R., Dobbins, M., Montalvo, V., Díaz, J.C. C., Montuy, G.P., Torre, J.A. de la, Brenes-Mora, E., Wood, M.A., Gilbert, J., Jetz, W., Miller, J.A., 2019. A sensitivity analysis of the application of integrated species distribution models to mobile species: a case study with the endangered Baird's tapir. Environ. Conserv. 46, 184–192. https://doi.org/10.1017/S0376892919000055.

Schmidt, J.I., Chapman, F., 2014. Relationship of community characteristics to harvest reporting: comparative study of household surveys and harvest tickets in Alaska. Hum. Dimens. Wildl. 19, 334–346. https://doi.org/10.1080/10871209.2014.917219.

Shipley, A.A., Sheriff, M.J., Pauli, J.N., Zuckerberg, B., 2019. Snow roosting reduces temperature-associated stress in a wintering bird. Oecologia 190, 309–321. https://doi.org/10.1007/s00442-019-04389-x.

Simmonds, E.G., Jarvis, S.G., Henrys, P.A., Isaac, N.J.B., O'Hara, R.B., 2020. Is more data always better? A simulation study of benefits and limitations of integrated distribution models. Ecography 43, 1413–1422. https://doi.org/10.1111/ecog.05146.

Townsend, Clare, J., Liu, N., Stenglein, J.L., Anhalt-Depies, C., Deelen, T.R.V., Gilbert, N. A., Singh, A., Martin, K.J., Zuckerberg, B., 2020. Integrating remote sensing and jurisdictional observation networks to improve the resolution of ecological management. bioRxiv. doi:https://doi.org/10.1101/2020.06.08.140848.

WDNR, 2020. Wisconsin wildlife reports - Wisconsin DNR [WWW Document]. URL. https://dnr.wi.gov/topic/wildlifeHabitat/reports.html (accessed 7.15.20).

Wearn, O.R., Glover-Kapfer, P., 2019. Snap happy: camera traps are an effective sampling tool when compared with alternative methods. R. Soc. Open Sci. 6, 181748 https://doi.org/10.1098/rsos.181748.

Wiens, J.A., Bachelet, D., 2010. Matching the multiple scales of conservation with the multiple scales of climate change. Conserv. Biol. 24, 51–62. https://doi.org/10.1111/j.1523-1739.2009.01409.x.

Wilson, E.C., Shipley, A.A., Zuckerberg, B., Peery, M.Z., Pauli, J.N., 2019. An experimental translocation identifies habitat features that buffer camouflage mismatch in snowshoe hares. Conserv. Lett. 12, e12614 https://doi.org/10.1111/conl.12614.

Zipkin, E.F., Inouye, B.D., Beissinger, S.R., 2019. Innovations in data integration for modeling populations. Ecology 100, e02713. https://doi.org/10.1002/ecy.2713.